$$-(\delta-1)/\delta=(1+db_r)/b_H\,. \qquad \text{(B6b)}$$

Combining (B3), (B4), and (B6), we obtain

$$\gamma'=\nu_\phi(2-\eta)\,, \qquad \text{(B7a)}$$

$$(\delta-1)/\delta=\mu_\phi(2-\eta)\,. \qquad \text{(B7b)}$$

---

*Work based in part on a Ph.D. thesis of L. L. Liu to be submitted to the Electrical Engineering Department of The Johns Hopkins University.

†Supported by Research Grant No. GP-15428 from the National Science Foundation, by the Office of Naval Research, and by the Air Force Office of Scientific Research

‡Present address: Physics Department, Room 13-2134, MIT, Cambridge, Mass. 02139.

[1]See, e.g., G. S. Rushbrooke, J. Chem. Phys. 39, 842 (1963); R. B. Griffiths, Phys. Rev. Letters 14, 623 (1965); J. Chem. Phys. 43, 1958 (1965). Recent reviews include R. B. Griffiths [in C. Domb and M. S. Green (unpublished)].

[2]B. Widom, J. Chem. Phys. 43, 3892 (1965); 43, 3898 (1965); C. Domb and D. L. Hunter, Proc. Phys. Soc. (London) 86, 1147 (1965); L. P. Kadanoff, Physics 2, 263 (1966); R. B. Griffiths, Phys. Rev. 158, 176 (1967), and references contained therein. See, E. Riedel, Phys. Rev. Letters 28, 675 (1972) and A. Hankey, H. E. Stanley, and T. S. Chang, Phys. Rev. Letters 29, 278 (1972) for the treatment of more complex systems (e.g., tricritical points).

[3]B. D. Josephson, Proc. Phys. Soc. (London) 92, 269 (1967); 92, 276 (1967).

[4]M. J. Buckingham and J. D. Gunton, Phys. Rev. 178, 848 (1969). Inequalities (5) were first proposed—but not proved rigorously—by G. Stell [Phys. Rev. Letters 20, 533 (1968)] and by J. D. Gunton and M. J. Buckingham [Phys. Rev. Letters 20, 143 (1968)].

[5]M. E. Fisher, Phys. Rev. 180, 594 (1969).

[6]See, e.g., the definitions of exponents and the general discussion in M. E. Fisher, Rept. Progr. Phys. 30, 615 (1967) and in H. E. Stanley, *Introduction to Phase Transitions and Critical Phenomena* (Oxford U.P., New York, 1971), Chaps. 3 and 4.

[7]M. A. Moore, D. Jasnow, and M. Wortis, Phys. Rev. Letters 22, 940 (1969).

[8]G. Stell, Phys. Rev. Letters 24, 1343 (1970); N. S. Snider, J. Chem. Phys. 54, 4587 (1971); A. Hankey and H. E. Stanley, Phys. Rev. B 6 (to be published). See also M. E. Fisher, J. Phys. Soc. Japan 26S, 87 (1969).

[9]R. B. Griffiths, J. Math. Phys. 8, 478 (1967); 8, 484 (1967); D. G. Kelly and S. Sherman, *ibid.* 9, 466 (1968); R. B. Griffiths, *ibid.* 10, 1559 (1969).

[10]See G. H. Hardy, J. E. Littlewood, and G. Polya, *Inequalities* (Cambridge U.P., London, 1959), 2nd ed., Theorem 16.

[11]Note that an unfortunate reversal of the inequality sign occurs in Fisher's statement of Lemma I (Ref. 5). We wish to thank Professor Fisher for having called this to our attention.

[12]Note that although Fisher (Ref. 5) uses $\phi=1$ in Eq. (2) [his Eq. (25)] to define the correlation length, he actually starts his derivation of the inequalities (5) from Eq. (11) [his Eq. (27)] by taking $\phi=0$. Hence although our ν_ϕ reduces to ν for $\phi=1$, our new inequalities reduce to old inequalities by taking $\phi=0$.

[13]A. Hankey and H. E. Stanley, see Ref. 8.

PHYSICAL REVIEW B VOLUME 6, NUMBER 5 1 SEPTEMBER 1972

Neutron-Diffraction Study of the Magnetic Structure of the Trirutile $LiFe_2F_6$

G. Shachar, J. Makovsky, and H. Shaked

Nuclear Research Center-Negev, P. O. Box 9001, Beer Sheva, Israel

(Received 7 September 1971)

A neutron-diffraction study of polycrystalline $LiFe_2F_6$ was performed. This compound is of the trirutile structure ($D_{4h}^{14}-P4_2/mnm$) and is paramagnetic at room temperature. The previously reported transition to antiferromagnetism at $T_N\sim105$ °K is confirmed. The magnetic structure was found to be collinear, with the spins parallel to the tetragonal axis. Nearest and next-nearest neighbors are coupled ferro and antiferromagnetically, respectively. The magnetic space group is $P4_2'/mnm'$. It is argued that this structure is to be expected on the basis of known data for the rutiles: MnF_2, FeF_2, and Fe-doped MnF_2. It was also found that at low temperatures the iron and fluorine ions are shifted from their room-temperature positions.

I. INTRODUCTION

The compound $LiFe_2F_6$ is a member of the family of compounds whose chemical formula can be written as $LiA^{+2}B^{+3}F_6$ (A, B, =transition metals). Several compounds of this family were investigated by Viebahn *et al.*[1,2] and were found to be of the trirutile structure. This structure belongs to the tetragonal space group $D_{4h}^{14}-P4_2/mnm$. X-ray studies by Portier *et al.*[3] showed that also $LiFe_2F_6$ is of the trirutile structure with $a=4.673$ Å and $c=9.290$ Å. Susceptibility measurements[3] showed that this compound undergoes a para to anti-ferromagnetic transition at $T_N\sim105$ °K. In the present work we report on the low-temperature magnetic structure and crystallographic distortion in

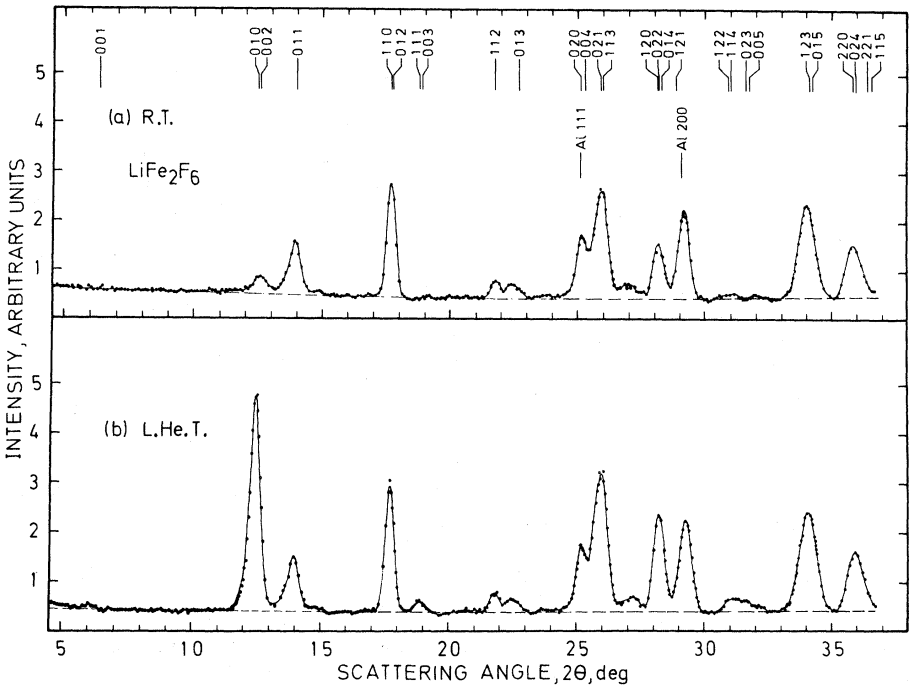

FIG. 1. Neutron- ($\lambda = 1.02$ Å) diffraction patterns of polycrystalline sample of $LiFe_2F_6$. The indexing is according to the tetragonal cell with $a = 4.673$ Å and $c = 9.290$ Å.

$LiFe_2F_6$ as determined by neutron diffraction.

II. EXPERIMENTAL

The material was prepared from LiF (British Drug Houses, Ltd. optran 47029), FeF_2 (Koch light 8366h), and FeF_3 (Koch light 8367h). Chemical analysis of the FeF_2 revealed the presence of about 27 mole% FeF_3, which was suitably taken into account in the preparation of the starting mixture. The stoichiometric mixture was heated up to 800 °C in an argon atmosphere. X-ray powder diagrams of the resulting material revealed all the lines observed by Portier *et al.*[3] Additional lines were observed with the following d values (in Å): 4.35, 3.03, 2.90, 2.62, 2.17, 2.13, 1.92, 1.75, and 1.38. These lines (except the 2.62-Å line) can be attributed to the presence of α-Li_3FeF_6.[2,4]

The neutron- ($\lambda \sim 1.02$ Å) diffraction patterns obtained at room temperature (RT) and at liquid-helium temperature (LHeT) are presented in Figs. 1(a) and 1(b), respectively. The two patterns are indexed according to the lattice constants reported by Portier *et al.*[3] Only a single weak line which does not belong to $LiFe_2F_6$ was observed at $2\theta \sim 27°$ ($d = 2.17$ Å). Comparison of Figs. 1(a) and 1(b) reveals that as the sample is cooled from RT to LHeT there is an increase in the intensities of the following four lines: {010}+{002}, {111}+{003}, {120}+{022}+{014}, and {122}+{114}. The peak-intensity-temperature curves of the first three of these lines exhibited a transition at about the reported[3] Néel temperature, $T_N \approx 105$ °K. The curve obtained for the strongest of the three lines, the line {010}+{002}, is shown in Fig. 2. This curve is similar to those usually found for magnetic lines, except for the absence of a sharp break in the slope at T_N. The "tail" above 105 °K can be accounted for by a crystallographic distortion and/or a short-range magnetic order (SRMO) and/or a

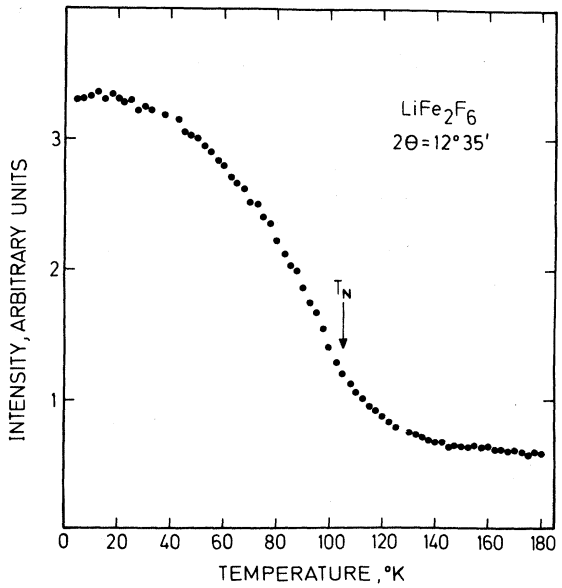

FIG. 2. Temperature dependence of the peak intensity of the {010}+{002} line in $LiFe_2F_6$. The Néel temperature $T_N = 105$ °K reported by Portier *et al.* (Ref. 3) is indicated.

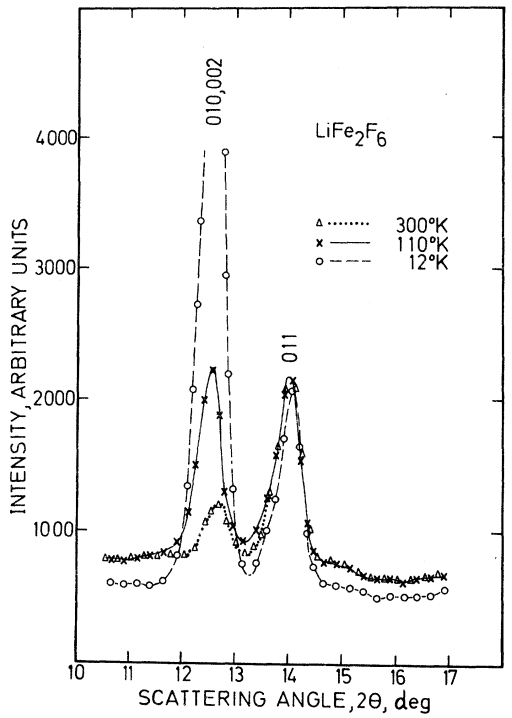

FIG. 3. Neutron-diffraction patterns of the {010} +{002} and {011} lines with the sample at 300, 110, and 12 °K.

partial long-range magnetic order (LRMO). A diffraction pattern observed just above T_N, at 110 °K, is compared in Fig. 3 with patterns observed at 300 and 12 °K. At 110 °K the {010}+{002} line is of same width as at the other temperatures and does not show the broadening characteristic of SRMO. Hence, the existence of SRMO at $T > T_N$ is excluded on the basis of this result. Furthermore, the background in the 12 °K pattern is about 25% lower than the background in the 300 and 110 °K patterns. This decrease is due to the build-up of magnetic order which causes the paramagnetic contribution to the background to diminish. The 110 °K background is practically the same as the 300 °K background, indicating that there is no more magnetic order (SRMO or LRMO) at 110 than at 300 °K. In order to compare the temperature dependence of the intensity of the {010}+{002} line with that predicted by molecular-field theory we plotted in Fig. 4 the function $[N(T) - N(T_N)]^{1/2}/[N(0) - N(T_N)]^{1/2}$ as the reduced magnetization vs T/T_N with $T_N \sim 105$ °K. $N(T)$ are the number of counts at temperature T. For $N(0)$ we have taken the number of counts at LHeT. The reduced magnetization predicted by the molecular field [average over the $j=2$ (Fe^{2+}) and the $j=\frac{5}{2}$ (Fe^{3+}) curves] is also given in Fig. 4. A plot of the same data but with $T_N \sim 115$ °K led to a reduced magnetization curve which deviated considerably from the molecular-field result. These results indicate that the contribution to the "tail" in Fig. 2 is of a crystallographic rather than a magnetic origin.

III. MAGNETIC STRUCTURE

The iron ions in $LiFe_2F_6$ occupy the $4e$ positions[3] $(0, 0, z)$, $(0, 0, \bar{z})$, $(\frac{1}{2}, \frac{1}{2}, \frac{1}{2}+z)$, $(\frac{1}{2}, \frac{1}{2}, \frac{1}{2}-z)$ in $P4_2/mnm$. The first and second (also third and fourth) iron ions are nearest neighbors (nn) and are related by an inversion. The first and fourth (also second and third) iron ions are next-nearest neighbors (nnn) and are related by a twofold screw axis. The 12 possible magnetic structures compatible with $P4_2/mnm$ are schematically shown in Fig. 5. These structures can be classified according to four basic configurations F^+, F^-, A^+, and A^-. F and A stand for ferro and antiferromagnetic coupling, respectively, between magnetic moments of nnn. + and − stand for ferro and antiferromagnetic coupling, respectively, between the magnetic moments of nn (configurations even and odd with respect to the inversion). The conditions limiting possible magnetic reflections from these configurations are listed in Table I. The magnetic reflections from these configurations are listed in Table I. The magnetic structure of $LiFe_2F_6$ will now be determined assuming that the three lines which have a transition temperature at about T_N (see Sec. II) contain magnetic contributions. According to Table I the appearance of the line {111} +{003} rules out the F^+ and F^- configurations and

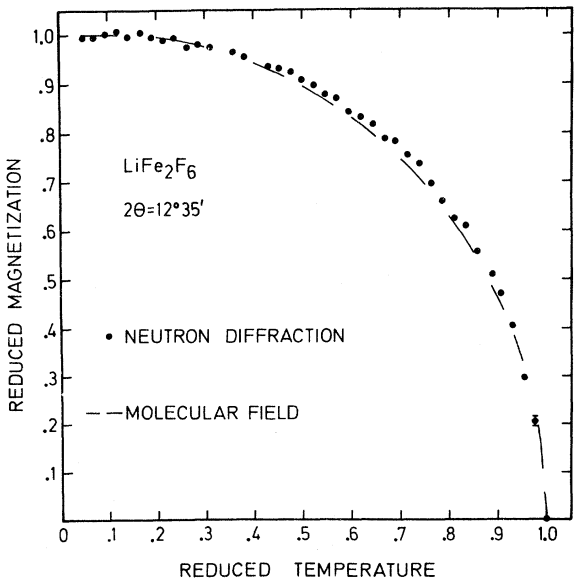

FIG. 4. Reduced temperature dependence of the reduced sublattice magnetization in $LiFe_2F_6$ derived from the observed {010}+{002} line. The molecular-field result ($J \sim \frac{3}{4}$) is also shown.

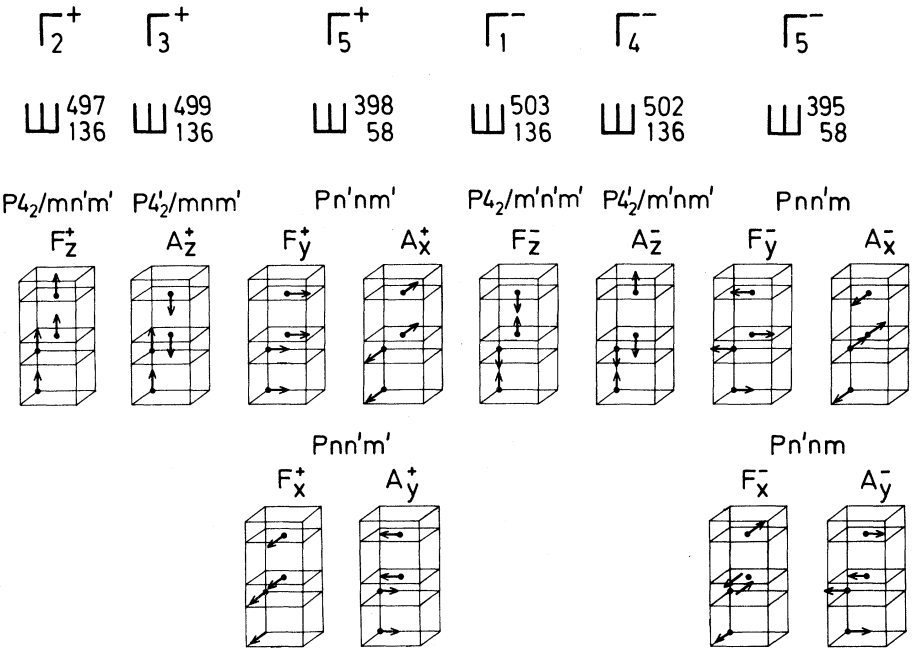

FIG. 5. Collinear magnetic structures at the 4*e* positions of 1′ $P4_2/mnm$, classified according to the irreducible representations with $\vec{k}=(0,0,0)$. The enumeration of the representations is according to the order in which they appear in Ref. 5. In the second and third lines the magnetic groups are given in the notation defined in Refs. 6 and 7, respectively.

requires that all nonzero magnetic reflections will satisfy the condition $h+k+l=2n+1$. Consequently, the first magnetic line should be assigned to the {010} reflection. This reflection is not allowed in the A^- configuration; hence, the configuration is A^+. The four lines listed in Sec. II should therefore be indexed as {010}, {111}+{003}, {120}+{014}, and {122}. The reflection {001} is allowed by the A^+ configuration but is absent in the diffraction pattern. This implies that the antiferromagnetic axis is parallel to z. We therefore conclude that A_z^+ is the only magnetic structure compatible with $P4_2/mnm$ and consistent with the line extinctions of the diffraction pattern. In Sec. IV we shall show that this structure is also consistent with the line intensities.

IV. REFINEMENT

A least-squares-refinement computer program was used to determine the four site parameters,[3] Debye-Waller constant,[8] and the number of Bohr magnetons which best fit the observed intensities. The observed integrated intensities, the parameters which yield the best fit, and the intensities calculated with these parameters are given in Tables II and III. The refined RT Debye-Waller constant, B, was -0.2 ± 1.0 Å^2, hence $B=0$ was used throughout refinements at all temperatures. The results given in Tables II and III can be summarized as follows: (a) For the RT data, agreement with x-ray results[3] is good except for the z parameter of 8*j* site (F^-). (b) $LiFe_2F_6$ may be visualized as a six-layer (packed along the c axis) structure: LiF_2, FeF_2, FeF_2, LiF_2, FeF_2, FeF_2. At RT, the layers are $\frac{1}{6}c$ apart. At 110 °K and LHeT the LiF_2 layers remain $\frac{1}{2}c$ apart, whereas neighboring FeF_2 layers are shifted closer to each other. (c) The nn distance of the iron ions is[10] 3.09 ± 0.07, 3.29 ± 0.09, and 3.44 ± 0.13 Å at RT, 110 °K ($\mu=0$), and LHeT, respectively. The nnn distance is[10] 3.65 ± 0.03, 3.57 ± 0.04, and 3.52 ± 0.04 Å at these temperatures, respectively. (d) The refined number of Bohr magnetons $\mu=(4.4\pm0.3)\,\mu_B$ at LHeT is very close to the 4.5 value expected for a 1:1 mixture of Fe^{2+} and Fe^{3+} ions. (e) In refining the 110 °K data we used two sets of parameters. In one set we fixed μ at 0. In the other set μ was allowed to vary and it converged to $\mu=1.6\mu_B$. The resulting R factors were about the same ($R\sim10\%$) for the two sets. Hence, in view of the arguments presented earlier in favor of no partial LRMO at 110 °K (Sec. II) we accept the result with $\mu=0$ as a representative of the physical situation.

We have also looked for a possible order of the divalent (or trivalent) iron ions among the 4*e* positions which will best fit the observed intensities

TABLE I. Limiting conditions on allowed reflections for the magnetic configurations of the 4*e* sites in $P4_2/mnm$.

Config.	l	$h+k+l$
F^+	...	$2n$
F^-	$\neq 3n$	$2n$
A^+	...	$2n+1$
A^-	$\neq 3n$	$2n+1$

TABLE II. Comparison of calculated[a] and observed[b] integrated intensities of neutrons reflected from a powder sample of $LiFe_2F_6$ at RT, 110 °K, and LHeT.

{hkl}	RT		110 °K			LHeT	
	I_{obs}	I_{calc} $\mu=0$	I_{obs}	I_{calc} $\mu=0$	I_{calc} $\mu=1.6\mu_B$	I_{obs}	I_{calc} $\mu=4.4\mu_B$
010,002	18 ± 2	21	49 ± 2	46	48	202 ± 3	198
011	75 ± 2	76	62 ± 2	67	66	68 ± 2	71
110	172 ± 2	169	152 ± 2	149	149	181 ± 2	182
111	0 ± 1	0	1 ± 3	3	7	25 ± 3	34
112	63 ±12	97	38 ±12	141	113	62 ±12	134
013	34 ± 8	11	47 ± 8	18	18	31 ± 8	24
020,004,021,113	538 ±15	562	536 ±15	538	564	629 ±15	655
120,022,014	310 ±30	441	257 ±30	378	391	434 ±20	424
122,114,023	29 ±15	105	66 ±15	41	81	149 ±30	161
123,015	1000 ±25	996	1000 ±25	937	925	1000 ±25	894
220,024,221,115	535 ±20	471	526 ±20	548	505	603 ±20	573

[a] $I_{calc}=j[F^2_{nuc}+q^2F^2_{mag}]$, see Ref. 9, p. 163. The refined parameters (Table III) and the form factor (Ref. 9) $f=e^{-0.05k^2}$, where $k=4\pi\sin\theta/\lambda$ were used in the calculations. The nuclear scattering amplitudes (Ref. 9) −0.18, 0.96, and 0.55 10^{-12} cm—were used for Li, Fe, and F, respectively.

[b] $I_{obs}=I_{nt}\sin\theta\sin2\theta$, where I_{nt} is the observed relative integrated intensity.

at LHeT, but found that the differences between ordered and disordered configurations were insignificant.

V. DISCUSSION

The results presented above prove that the magnetic structure of $LiFe_2F_6$ is A_z^+ (Fig. 5), corresponding to the magnetic group $P4_2'/mnm'$. It was pointed out by Portier *et al.*[3] that this structure is expected in $LiFe_2F_6$ if one assumes the same interactions in $LiFe_2F_6$ as in FeF_2. Antiferromagnetic ordering was also observed in several other trirutile compounds. In terms of the notation of Fig. 5 their magnetic structures are[11–13] A_x^- (or A_y^-) for Cr_2TeO_6 and possibly for $(FeCr)WO_6$, F_x^- (or F_y^-) for Cr_2WO_6 and possibly for V_2WO_6, A_z^- for Fe_2TeO_6. Hence the magnetic structure of the trirutile fluoride $LiFe_2F_6$ is different from the magnetic structure observed in oxides of the trirutile structure.

It is of interest to compare $LiFe_2F_6$ (trirutile) with FeF_2 and other (rutile) fluorides. In Table IV we present such a comparison. Since $LiFe_2F_6$ contains both divalent ($3d^6$) and trivalent ($3d^5$) iron ions, the comparison is made with FeF_2 ($3d^6$ ions), MnF_2 ($3d^5$ ions), and Fe-doped MnF_2 ($3d^5$ and $3d^6$ ions). $LiFe_2F_6$ and these rutile fluorides belong to the same space group and the interionic distances are very nearly the same. These rutile fluorides are antiferromagnetic. In all of them nn are coupled ferromagnetically, whereas nnn coupled antiferromagnetically. The corresponding energies of the exchange interactions are presented in Table IV. In $LiFe_2F_6$ the following nn and nnn interactions are to be expected: $3d^5$-$3d^5$, $3d^6$-$3d^6$, and $3d^5$-$3d^6$. It seems plausible that these inter-

TABLE III. Parameters for $LiFe_2F_6$ ($D_{4h}^{14}-P4_2/mnm$) refined with the RT, 110 °K, and LHeT data. Final R factors[a] and RT x-ray results (Ref. 3) are also given.

Ion	Site	Param.	X rays (Ref. 3) RT	Neutrons RT	110 °K		LHeT
Fe^{2+}, Fe^{3+}	4e	z	0.333	0.334 ±0.004	0.323 ±0.005	0.328 ±0.007	0.315 ±0.007
F^-	4f	x	0.305	0.306 ±0.007	0.298 ±0.010	0.298 ±0.009	0.306 ±0.009
F^-	8j	x	0.305	0.319 ±0.004	0.313 ±0.007	0.313 ±0.007	0.295 ±0.012
F^-	8j	z	0.333	0.335 ±0.0051	0.319 ±0.005	0.328 ±0.010	0.320 ±0.009
μ_B			0[b]	0[b]	0[b]	1.6 ±0.6	4.4 ±0.3
Weighted R factors			0.11[c]	0.082	0.105	0.092	0.063

[a] $R=\{\Sigma[(I_{obs}-I_{calc})/\sigma]^2/\Sigma[I_{obs}/\sigma]^2\}^{1/2}$, the σ's are the estimated errors in I_{obs} and are listed in Table II.

[b] Here μ_B was set equal to zero throughout the refinement.

[c] The factor obtained with the x-ray parameters and with the RT neutron data is 0.15; the value 0.11 was reported by Portier *et al.* (Ref. 3) for their x-ray data.

TABLE IV. Pertinent data for $LiFe_2F_6$, FeF_2, MnF_2, and MnF_2:Fe.

Compound	a (Å)	c (Å)	z Fluor	Electron configuration	J_{nn} (°K)	J_{nnn} (°K)	T_N (°K)	Ref.
$LiFe_2F_6$	4.673	9.29	0.305	$3d^5, 3d^6$			105	3
FeF_2	4.697	3.31	0.305	$3d^6$	0.07	−5.2	78	14,15
MnF_2	4.873	3.31	0.310	$3d^5$	0.32	−1.76	67	14,16
MnF_2:Fe	4.873	3.31	0.310	$3d^5, 3d^6$	3.1[a]	−3.3[a]	varies	17,18

[a]These exchange interactions correspond to the Mn:Fe interaction in these samples.

actions will not differ markedly from the corresponding interactions in the rutile fluorides. Since in the rutile fluorides all three J_{nn} are positive and all three J_{nnn} are negative, it is to be expected that also in $LiFe_2F_6$ $J_{nn} > 0$ and $J_{nnn} < 0$. The magnetic configuration of $LiFe_2F_6$ is, in fact, in full accord with these considerations since the spin magnetizations of nn and nnn are parallel and antiparallel, respectively.

The direction of the magnetization in the rutile fluorides is parallel to z. In MnF_2 the magnetic ions are in the S state and the spin direction is consequently determined mostly by the dipolar fields.[19] In FeF_2, however, the dipolar contribution is small compared to the single-ion anisotropy of the Fe ions.[15,20] It is to be expected therefore that the single-ion anisotropy of the $3d^6$ ions will favor the z direction in $LiFe_2F_6$ as well. We have, nevertheless, calculated the dipolar field in $LiFe_2F_6$ with Fe^{2+}, Fe^{3+} randomly distributed on the 4e sites. The field was found to be parallel to z and about 3300 Oe in magnitude. Thus observed spin direction in $LiFe_2F_6$ is in full accord with these considerations. The fact that J_{nn} is much greater for unlike ions than for like ions (Table IV) suggests that in the magnetically ordered state nearest neighbors will be in pairs of Fe^{2+} and Fe^{3+}. Portier *et al.*[3] established that $LiFe_2F_6$ is not ferrimagnetic. They suggested that this indicates that Fe^{2+} and Fe^{3+} are distributed randomly. It should be noted however that an A_z^+ structure with ordered pairs of Fe^{2+} and Fe^{3+} as nn is compatible with the absence of ferrimagnetism. Comparing T_N of $LiFe_2F_6$ with T_N of the rutile fluorides we note[18] that for $Mn_{1-x}Fe_xF_2$, T_N has a maximum at $x = 0.75$. This is attributed[18] to the fact that for unlike ions J_{nn} is much greater than for like ions. The maximal T_N for $Mn_{1-x}Fe_xF_2$ is about 79 °K, which is considerably lower than 105 °K—the Néel temperature of $LiFe_2F_6$. This fact indicates that a straightfoward quantitative deduction from the rutile fluorides to $LiFe_2F_6$ is not applicable. One of the factors which must be considered for $LiFe_2F_6$ is a possible hopping of the electrons which may give rise to double-exchange interactions.[21] This hopping can occur when ions of different valencies occupy otherwise equivalent positions (4e in our case). As an example we cite Eu_3S_4 (T_d^6-$I\bar{4}3d$) in which one Eu^{2+} and two Eu^{3+} occupy equivalent positions (12a). Mössbauer spectroscopy[22] along with electrical conductivity and thermal emf measurements[23] showed that electron hopping is in fact taking place in Eu_3S_4. In order to establish whether electron hopping is occurring also in $LiFe_2F_6$ similar measurements are presently underway in our laboratory.

Note added in proof. While the present work was in press, the magnetic structure of $LiFe_2F_6$ was reported in a communication by M. Wintenberger, M. A. Tressaud, and F. Menil [Solid State Commun. 10, 739 (1972)]. The magnetic structure reported here is in complete agreement with the structure reported there.

ACKNOWLEDGMENT

Many discussions with Professor S. Shtrikmann of the Weizmann Institute of Science are gratefully acknowledged.

[1]W. Viebahn, W. Rudorff, and H. Kornelson , Z. Naturforsch. 22b, 1218 (1967).

[2]W. Viebahn, W. Rudorff, and R. Hansler, Chimia 23, 12, 503 (1969).

[3]J. Portier, A. Tressaud, R. De Pape, and P. Hagenmuller, C. R. Acad. Sci. (Paris), Serie C t267, 1711 (1968).

[4]A. Tressaud, thesis (University of Bordeaux, 1969) (unpublished).

[5]G. F. Koster, in *Solid State Physics*, edited by F. Seitz and D. Turnbull (Academic, New York, 1957), Vol. 5, p. 191.

[6]V. A. Koptsik, *Shubnikov Groups* (Moscow State U. P., Moscow, 1966) (in Russian).

[7]W. Opechowski and R. Guccione, in *Magnetism*, edited by G. T. Rado and H. Suhl (Academic, New York, 1965), Vol. IIa, p. 105.

[8]The Debye-Waller constant B is defined by $I_{obs} = I_{calc} \times e^{-B/2d^2}$, where $d = \lambda/2 \sin\theta$.

[9]G. E. Bacon, *Neutron Diffraction* (Oxford U. P., Oxford, England, 1962).

[10]The nn and nnn distances are given by $d_{nn} = (1 - 2z)\, c$ and $d_{nnn} = \frac{1}{2}[2 + (4z-1)^2 c^2/a^2]^{1/2} a$ with $\Delta d_{nn} \sim 2c\Delta z$ and $\Delta d_{nnn} \sim c^2(4z-1)\, \Delta z/d_{nnn}$.

[11]W. Kunnmann, S. La Placa, L. M. Corliss, J. M. Hastings, and E. Banks, J. Phys. Chem. Solids 29, 1359

(1968).
[12]M. C. Montmory and R. Newnham, Solid State Commun. 6, 1359 (1968).
[13]M. C. Montmory, M. Belakhovsky, R. Chevalier, and R. Newnham, Solid State Commun. 6, 317 (1968).
[14]H. J. Guggenheim, M. T. Hutchings, and B. D. Rainford, J. Appl. Phys. 39, 1120 (1968).
[15]J. W. Stout and S. A. Reed, J. Am. Chem. Soc. 76, 5279 (1954).
[16]A. Okazaki, K. C. Turberfield, and R. W. H. Stevenson, Phys. Letters 8, 9 (1964).
[17]M. Butler, V. Jaccarino, N. Kaplan, and H. J. Guggenheim, Phys. Rev. B 1, 3085 (1970).
[18]G. K. Wertheim, H. J. Guggenheim, M. Butler, and V. Jaccarino, Phys. Rev. 178, 804 (1969).
[19]F. Keffer, Phys. Rev. 87, 608 (1952).
[20]M. E. Lines, Phys. Rev. 156, 543 (1967).
[21]See, e. g., P. W. Anderson, in *Magnetism*, edited by G. T. Rado and H. Suhl (Academic, New York, 1963), Vol. I.
[22]O. Berkooz, M. Melamud, and S. Shtrikman, Solid State Commun. 6, 185 (1968).
[23]I. Bransky, N. M. Tallan, and A. Z. Hed, J. Appl. Phys. 41, 1787 (1970).

PHYSICAL REVIEW B VOLUME 6, NUMBER 5 1 SEPTEMBER 1972

Magnon Heat Conduction and Magnon Scattering Processes in Fe-Ni Alloys*

W. B. Yelon† and L. Berger
Physics Department, Carnegie-Mellon University, Pittsburgh, Pennsylvania 15213
(Received 3 January 1972; revised manuscript received 19 April 1972)

The thermal and electrical conductivities of 70-wt%-Ni–30-wt%-Fe, 81-wt%-Ni–19-wt%-Fe, and 67-wt%-Ni–33-wt%-Cu have been measured between 1.5 and 4.5 K, in external fields up to 6 T. Both nickel-iron alloys show a small magnon contribution κ_m to the thermal conduction, equal to about 3% of the total conductivity at 4 K. In 70-wt%-Ni–30-wt%-Fe $\kappa_m \propto T^{1.9}$ is found. Using a simple kinetic-theory model, the magnon lifetime τ_m is derived equal to 1.7×10^{-10} sec at 4 K and varying as $T^{-0.6}$. This implies $\tau_m \propto \omega^{-0.6}$. In the zero-magnetostriction alloy 81-wt%-Ni–19-wt%-Fe, $\kappa_m \propto T^{1.5}$ and $\tau_m \propto T^{-1} \propto \omega^{-1}$ is found to hold. Our lifetime values agree with those derived from magnetic resonance linewidths. The nickel-copper alloy shows no magnon heat transport, implying a magnon lifetime of less than 2×10^{-11} sec at 3.55 K. Shorter magnon lifetime in Ni-Cu than in Ni-Fe may reflect faster magnon-electron relaxation, corresponding to increased smearing of the electron momentum gap by alloy disorder. The latter correlates, in turn, with larger electrical resistivity and smaller magnetization.

I. INTRODUCTION

Magnons can be expected to carry a sizable heat current in any ferromagnetic or antiferromagnetic material if the magnon lifetime is long enough. This magnon conduction has been observed in insulators, both ferro-[1,2] and antiferromagnetic.[3,4] There is also evidence of magnon conduction in ferromagnetic rare earths,[5] but there have been no similar reports for transition metals. This is because the separation of the magnon contribution from that of the electrons and phonons has been a very difficult problem. However, in concentrated alloys we expect that the magnon contribution may be seen because of its distinctive field dependence, the electron and phonon contributions being essentially field independent above saturation.

This work is an investigation of three ferromagnetic alloys, 70-wt%-Ni–30-wt%-Fe, 81-wt%-Ni–19-wt%-Fe, and 67-wt%-Ni–33-wt%-Cu. The thermal conductivity was measured in the temperature range 1.5–4.5 K, in magnetic fields up to 6 T. A preliminary report on this piece of research has already been published.[6]

II. ELECTRON AND PHONON THERMAL CONDUCTION

In our concentrated alloys at $T < 4$ K, electrons are scattered mostly by impurities. For example, we have checked that the electrical resistivity ρ of 81-wt%-Ni–19-wt%-Fe is constant to better than ±0.2% between 1.5 and 4.2 K, in a constant field of 0.715 T. Since this scattering is elastic, the Wiedemann-Franz law is expected to hold,[7] even in a magnetic field:

$$\kappa_e = \frac{\pi^2 k_B^2}{3e^2\rho} T ,$$

where κ_e is the electronic thermal conductivity and k_B the Boltzmann constant. Thus we can calculate κ_e from the measured ρ value. In concentrated alloys, ρ and κ_e are actually found to change very little above ferromagnetic saturation. This happens because $\omega_c\tau \ll 1$, where ω_c is the electron cyclotron frequency.

These alloys show a ferromagnetic anisotropy of the resistivity; that is, their electrical and thermal resistivities change considerably from zero applied field to technical saturation.[8] In